

Active Oxygen and Solid Alkali Pretreatment of Bamboo Residue: Features of Hemicellulose during the Cooking Process

Juan Du,^a Caixia Xiong,^a Bin Luo,^a Yong Sun,^{a,b,*} Xing Tang,^a Xianhai Zeng,^a Tingzhou Lei,^c Shijie Liu,^d and Lu Lin^{a,b,*}

Bamboo residue was treated with an active oxygen (O₂) and solid alkali (MgO) (CAOSA) process, which was developed recently by the authors owing to its environmentally friendly and high-efficiency characteristics. During the cooking process, 93.0% of lignin and 62.1% of hemicellulose were removed from the raw material, which resulted in a cellulose-rich pulp. This indicated that this cooking process is efficient to fractionate the bamboo residue into cellulose, hemicellulose, and lignin as a pretreatment for biomass conversion. The structural features of the hemicellulose from the pretreated bamboo residue were analyzed for comparison with that of the raw materials. The molecular structure of the hemicellulose fractions obtained from both the raw bamboo and pulp consisted of a (1→4)-β-D-Xylp backbone substituted with α-L-Araf and 4-O-methyl-α-D-glucuronic acid. The hemicellulose with more side chains tended to be more easily removed from the bamboo cell wall during the CAOSA process. Furthermore, the fractions of hemicellulose exhibited much lower thermal stabilities after the cooking process than the raw material.

Keywords: Active oxygen; Solid alkali; Pretreatment; Hemicellulose; Structural features

Contact information: a: College of Energy, Xiamen University, Xiamen, 361102, P. R. China; b: Xiamen Key Laboratory of High-valued Conversion Technology of Agricultural Biomass, 361102, P. R. China; c: Henan Key Laboratory of Biomass Energy, Huayuan Road 29, Zhengzhou, Henan 450008, P. R. China; d: Department of Paper and Bioprocess Engineering, State University of New York College of Environmental Science and Forestry, Syracuse, New York 13210, United States; * Corresponding authors: sunyong@xmu.edu.cn; lulin@xmu.edu.cn

INTRODUCTION

There has been a rapid depletion of fossil fuels, especially in recent decades, and the continuous release of pollutants from their combustion have propelled the development of research into the field of alternative and sustainable energy resources (Huber *et al.* 2006). Among these resources, biomass is renewable in nature and is capable of storing solar energy through photosynthesis in the form of cell wall polymers, which include cellulose, hemicellulose, and lignin (Ruiz *et al.* 2008; Wang *et al.* 2013). As the most abundant polysaccharide after cellulose in lignocellulosic materials, hemicelluloses are heteropolysaccharides that consist of different kinds of sugar units, such as xylose, arabinose, galactose, mannose, glucose, glucuronic acid, 4-O-methyl-D-glucuronic acid, and galacturonic acid.

Bamboo is one of the most important sources of biomass because of its fast growth, wide distribution, relatively high content of hemicellulose (22% to 35% pentosans in dry bamboo), and sustainable availability, and as such, it has attracted more and more attention recently (Liese 1987; Scurlock *et al.* 2000; Wen *et al.* 2011; Peng and She 2014). At

present, bamboo is used in reinforcing fibers, paper, textiles, and construction boards (Scurlock *et al.* 2000), which generates a large amount of residue and results in a waste of resources. Meanwhile, bamboo resources are relatively rich in East and Southeast Asia, especially in Fujian Province, China. However, the natural recalcitrance of bamboo lignocellulose makes it difficult to be converted into fuels, power, heat, and value-added chemicals. Although a variety of pretreatment methods, including physical, biological, chemical, and combination pretreatments, have been used in the biomass materials biorefinery process, leading lignocellulose pretreatment technologies still suffer from severe reaction conditions, the possibility of serious pollution, narrow substrate applicability, low reaction efficiency, and high capital investment (Wyman *et al.* 2005; Leenakul and Tippayawong 2010). Therefore, it is imperative to explore an efficient, environmentally friendly, and cost-competitive way to pretreat bamboo residue for biorefinery processes.

In an effort to reduce cost and pollution, a cooking process involving active oxygen and solid alkali (CAOSA) was developed by the authors (Pang *et al.* 2012). In the conventional industrialized cooking process, the NaOH, Na₂S, SO₂, and sulfite are often used as the cooking chemicals, while only active oxygen (O₂) and solid alkali (MgO) are used in the CAOSA process. Therefore, the CAOSA process with O₂ and MgO could significantly reduce, and even eliminate the pollution caused by the cooking chemicals. In this process, active oxygen is used to remove the lignin, and the solid alkali, which is slightly soluble in water, provides a weak alkaline condition to support delignification and protect the carbohydrates from carbonizing and hydrolyzing (Shi *et al.* 2012a). In comparison with other conventional cooking processes, the CAOSA process is an efficient and environmentally friendly biomass pretreatment method. Furthermore, the solid alkali (MgO) can be recycled in this process (Jiang *et al.* 2017). In addition, the CAOSA process was capable of removing a large amount of lignin (95.3%) and most of the hemicellulose, which resulted in a cellulose-rich pulp from bagasse (Shi *et al.* 2012b). Until now, the three separation components of bamboo residue in this process have not been well understood, and less attention has been paid to the chemistry and application of the hemicellulose in the bamboo pulp.

In the present study, the bamboo residue was first treated with the CAOSA process. In comparison with the low hemicellulose yield of corn stalk pulp (12% in pulp) (Shi *et al.* 2014), a relatively high hemicellulose yield in the bamboo pulp (20% in pulp) is retained in the CAOSA process. It is crucial to clarify the structural characterizations of bamboo hemicellulose for the further development of high value-added products. The chemical and structural changes of the hemicellulose involved in the CAOSA process were determined to give some insight for further utilization. Because of the complex hetero-polysaccharide structure of the bamboo residue hemicellulose, it was extracted and characterized by diverse methods.

EXPERIMENTAL

Raw Material and Active Oxygen Cooking Process

The bamboo residue from Mu-Jiang-Wei-Hua Perfumery Plant (Jiangmen, China) was dried initially in the oven and then cut into small pieces by a crusher. Its size was 20 mesh and the shape was chip (Fig. 2, (left)). Our previous study described the active oxygen cooking process (Shi *et al.* 2012a, 2012b; Yang *et al.* 2012; Jiang *et al.* 2017). The detailed

operations were as follows: 1 kg of bamboo residue (oven-dried weight) and 150 g of MgO were placed in a 22 L rotating ball-shaped digester with a solid-to-liquid ratio of 1:5 (w/v) with 10 cm diameter circular feed port by manual. After being sealed, the autoclave was filled with oxygen until a pressure of 1.0 MPa was achieved.

The constant heating rate was 2.1 °C/min, and the heating time to the target temperature was within 70 min. The cooking was performed at 165 °C for 3 h. After cooking, the yellow liquid was extruded from the raw stock and stored in a refrigerator. The remaining bamboo pulp was washed three times using deionized water and then air-dried. The main chemical compositions of the raw material and air-dried pulp material were evaluated according to the TAPPI standards for cellulose and hemicelluloses TAPPI T249 cm-00 (2000), Klason soluble and insoluble lignin TAPPI T222 om-02 (2002), and ash TAPPI T211 om-93 (1993). The loss rates of cellulose, hemicellulose, and lignin were calculated according to Eq. 1:

$$\text{Loss rate (\%)} = 1 - \frac{Y \cdot C_P}{C_R} \quad (1)$$

where Y is the yield of the pulp (%), C_P is the content of cellulose, hemicellulose, or lignin in the bamboo pulp (%), and C_R is the content of cellulose, hemicellulose, or lignin in the bamboo residue raw material (%).

Extraction of Hemicellulose

As shown in Fig. 1, the alkali-soluble hemicellulose was extracted from the de-waxed bamboo residue sample. The sample was delignified with 5% sodium chlorite in acidic solution (pH 3.8 to 4.0) at 75 °C for 2 h. The white insoluble residue was filtered and washed using water, followed by ethanol (75%). The residue was oven-dried at 55 °C for 16 h to obtain holocellulose. Because of the low lignin content in the bamboo pulp, it was used directly to extract hemicellulose. The holocellulose sample was extracted with 10% KOH at 25 °C for 16 h with a solid-to-liquid ratio of 1:25 (g/mL). The filtrate was adjusted to a pH of approximately 5.5 to 6.0 with acetic acid. The water-insoluble hemicellulose fractions from bamboo residue (BIF) and bamboo pulp (PIF) were recovered by centrifugation at 5,000 rpm for 5 min (Bendahou *et al.* 2007). The supernatant was concentrated under vacuum, poured into three volumes of 95% ethanol, and then was left overnight. After centrifugation at 4,000 rpm for 10 min, the precipitated hemicellulose was thoroughly washed using 75% ethanol and then freeze-dried. Finally, the water-soluble hemicellulose fractions from the bamboo residue (BSF) and bamboo pulp (PSF) were obtained (Bendahou *et al.* 2007).

Physiochemical Characterization of the Hemicellulose

Sugar compositional analyses

The monomeric sugars in the hemicellulose fractions were obtained from the hydrolysis of the hemicellulose. A hemicellulose sample of 5 mg was put in a pressure-resistant bottle. To 0.125 mL of 72% H₂SO₄, 1.35 mL of deionized water was added. The mixture was hydrolyzed at 105 °C for 2.5 h by shaking the bottle every 30 min. After hydrolysis, the sample was diluted 2,000-fold, filtered, and injected into a high-performance anion exchange chromatograph (Dionex, ICS-3000, Sunnyvale, CA) using pulsed amperometric detection (HPAEC-PAD) with an AS50 auto-sampler and a CarboPac PA-20 column (4 mm × 250 mm, Dionex). The neutral sugars were separated in 1 mM NaOH for 17 min, and then the column was washed using 250 mM NaOH for 10 min to

remove the carbonate. This was followed by a 5 min elution with 1 mM NaOH to re-equilibrate the column before the next injection. The whole process was performed at 30 °C with a flow rate of 0.7 mL/min. The uronic acid in the hemicellulose fractions was determined by p-hydroxybiphenyl colorimetry at 525 nm (Blumenkrantz and Asboe-Hansen 1973). Glucuronic acid was used as an external standard.

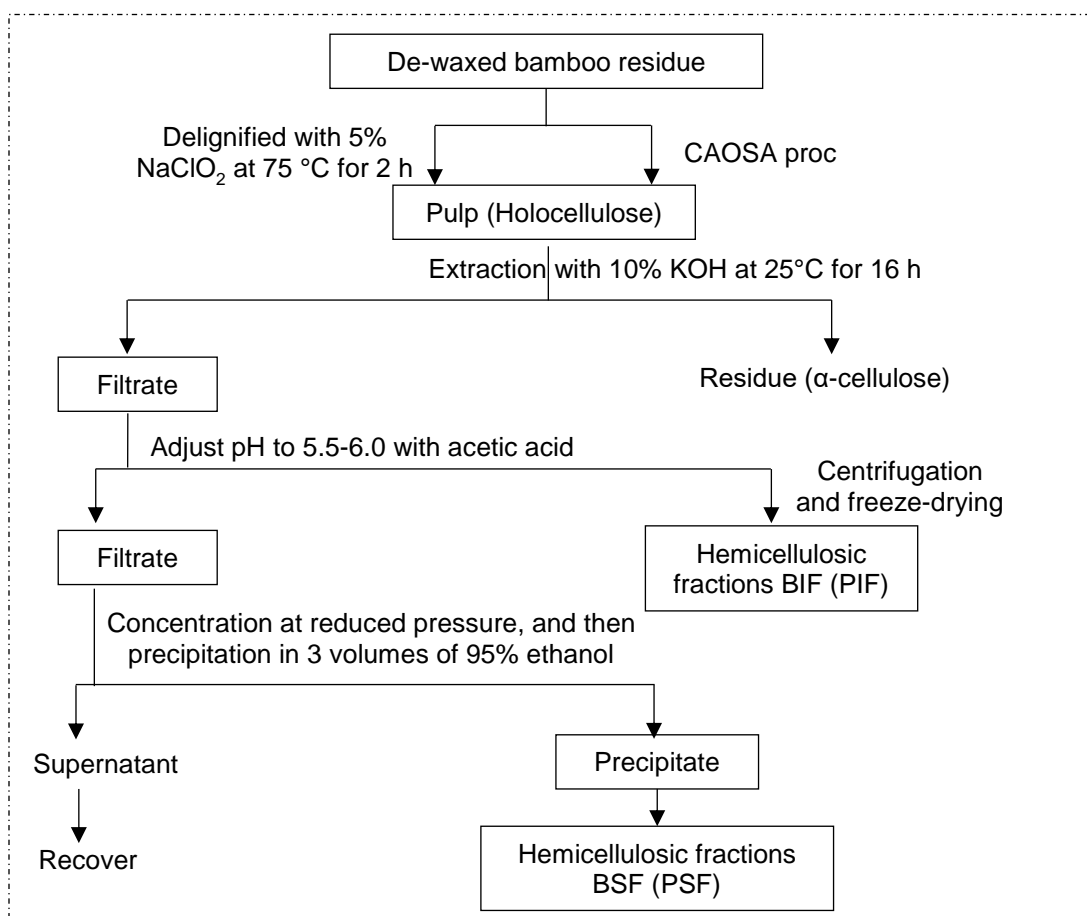


Fig. 1. Scheme for isolation of hemicelluloses from bamboo residue and pulp

Fourier-transform infrared spectroscopy (FT-IR) analysis

Fourier-transform infrared (FT-IR) spectra were obtained with a spectrophotometer (Bruker Tensor 27, Ettlingen, Germany). The samples were combined with KBr in slices containing 1% hemicellulose. A total of 32 scans were taken for each sample and were recorded from 4,000 to 400 cm^{-1} in the transmission mode.

Nuclear magnetic resonance (NMR) analysis

The solution-state nuclear magnetic resonance (NMR) spectra were obtained with an Ascend™ 600 MHz spectrometer (Bruker Biospin GmbH, Rheinstetten, Germany) at 25 °C. The hemicellulose sample (10 mg for ^1H and 80 mg for ^{13}C) was dissolved in 1 mL of DMSO- d_6 (δ H 2.5; δ C 39.52). The ^1H NMR spectra were recorded after 256 scans. A 2.73 s acquisition time, 10.64 μs pulse width, and 1.00 s relaxation delay time between scans were used. The ^{13}C NMR spectra were obtained at 25 °C after 10,000 scans. A 30° pulse flipping angle, 0.91 s acquisition time, 12.42 μs pulse width, and 2.00 s relaxation

delay time between scans were used. The ^1H - ^{13}C hetero-nuclear single quantum coherence (HSQC) spectra of the hemicellulose (60 mg in 1 mL $\text{DMSO-}d_6$) were obtained in the HSQC experiment mode at 25 °C. The spectral widths were 12,019 and 30,120 Hz for the ^1H and ^{13}C dimensions, respectively. The acquired time per scan was 0.04 s, the relaxation delay time was 2 s, and the pulse width was 10.64 μs .

Thermogravimetric analysis (TGA)

The thermogravimetric analysis (TGA) of the hemicellulose fractions was performed using a Leading Thermal Analysis (STA 449 F5, NETZSCH, Bavaria, Germany). A hemicellulose sample of approximately 10 mg was evenly distributed in a platinum crucible and heated from room temperature to 600 °C at a heating rate of 10 °C/min with a high-purity nitrogen gas flow rate of 50 mL/min.

RESULTS AND DISCUSSION

Chemical Composition

The morphologies of the bamboo residue and pulp before and after the cooking process are shown in Fig. 2. The morphology of the bamboo residue was completely changed to a fluffy state after cooking for 3 h at 165 °C. Its color had faded after the cooking pretreatment as well. Previous studies on the structural features of hemicellulose from corn stalk at different cooking stages indicated that the active oxygen cooking process is a moderate pretreatment procedure compared with the chemical cooking process (Shi *et al.* 2014). During the active oxygen cooking process, the gaseous oxygen did not directly react with the raw material. First, a small amount of molecular oxygen dissolved in the water forming active ions under the cooking conditions. Then, the active ions entered the water-soaked cell wall and broke the linkages between and among the main components.



Fig. 2. Photographs of the bamboo residue (left) and pulp (right)

The yields of pulp and content of each component in the bamboo residue and pulp are shown in Table 1. Most of the lignin (93.0%) was removed during the cooking process. This demonstrated that the CAOSA process is an efficient pretreatment method for biomass separation, and the active oxygen showed high selectivity for lignin. Compared with the lignin, the cellulose suffered a limited amount of loss during this process. Despite the fact that the hemicellulose had a certain degree of loss, the reserved hemicellulose in the

bamboo pulp (19.4%) was higher than that in the corn stalk (12.7%) and bagasse (13.1%) pulp by the same pretreatment process (Shi *et al.* 2012a, 2012b). This higher hemicellulose content is beneficial for further applications to obtain a variety of high-value-added products, such as xylose, xylitol, and xylo-oligosaccharides (XOS), without being obstructed by undesirable lignin.

Table 1. Main Components of the Bamboo Residue and Bamboo Pulp

Materials	Cellulose (%) ^a	Hemicellulose (%)	Lignin (%)	Ash (%)	Yield (%)
Bamboo residue	41.2	22.9	22.7	1.0	-
Bamboo pulp	75.3 (18.3) ^b	19.4 (62.1)	3.6(93.0)	0.9	44.7

^a Values based on the oven-dried weight; ^b The data in parentheses show the loss rates of cellulose, hemicellulose, and lignin during the cooking process.

Yield and Monomer Compositions of Different Hemicellulose Fractions

As shown in Table 2, the yields of hemicellulose from the bamboo residue and bamboo pulp were 43.9% and 21.4%, respectively. This result indicated that the extraction of hemicellulose from the bamboo pulp was more difficult than from the bamboo residue under these extraction conditions. The speculative reasons are as follows: (1) there is no significant difference of the hemicellulose content in bamboo pulp (19.4%) and the bleached bamboo residue (26.2%, data not shown); (2) some easily oxidized hemicellulose in the bamboo residue was dissolved into the yellow liquid during the CAOSA process. The phenomenon of hemicellulose loss was also indicated by the relatively low hemicellulose residual content (37.9%) from bamboo pulp in the CAOSA process (Table 1). As mentioned above, these results clearly showed that the active oxygen could not only efficiently remove subtotal lignin, but also oxidize the part hemicellulose during the cooking process.

Table 2. Monosaccharide Compositions in the Hemicellulose Fractions

Fractions ^a	Yield ^b (%)	Sugar composition (%)						Molar ratio ^c	
		Ara	Gal	Glu	Xyl	Man	Uro	Ara/Xyl	Uro/Xyl
BIF	37.4	4.1	0.4	1.8	92.6	ND	1.1	0.04	0.01
BSF	6.5	9.2	2.3	6.2	76.7	ND	5.5	0.12	0.06
PIF	20.3	3.0	0.3	1.9	93.6	0.6	0.6	0.03	0.00
PSF	1.1	2.0	0.5	56.9	36.2	0.3	4.1	0.05	0.09

^a BIF (PIF): Water-insoluble fractions from bamboo (pulp); BSF (PSF): Water-soluble fractions from bamboo (pulp); ^b BIF and BSF based on bleached bamboo residue, PIF and PSF based on bamboo pulp(wt.%); ^c Expressed in relative molar percentages; ND: not detected

The monosaccharide compositions are shown in Table 2. High contents of xylose in the BIF, BSF, and PIF were indicated in comparison to the PSF. Conversely, low contents of glucose in the BIF, BSF, and PIF were indicated relative to that of the PSF. The content percentage of arabinose in the four fractions was lower than 10.0%. Additionally,

the content percentage of the other monosaccharides in the four fractions, such as galactose, mannose, and uronic acid (glucuronic acid and/or galacturonic acid), seemed a little low (Table 2). These data suggested that the hemicellulose from bamboo was composed of glucuronoarabinoxylan-type polysaccharides, which is in agreement with previous studies (Maekawa 1976; Peng *et al.* 2011a, b; Wen *et al.* 2011).

Intriguingly, the glucose content (56.9%) was higher than the xylose content (36.2%) in the PSF. This might be due to the fact that the primary crystalline structure of bamboo residue was obstructed by lignin, hemicelluloses, *etc.*, whereas CAOSA process solubilized lignin and some hemicellulose (Kim *et al.* 2011). Then the crystalline structure of the cellulose became exposed and looser, and subsequently, the water-soluble glucose oligomers in the cellulose were released during the process of extracting hemicellulose from the bamboo pulp. Research into the enzymatic hydrolysis (cellulase and cellobiase) of the solid bagasse pulp treated by the CAOSA process showed that the high sugar yield (82.4%) was obtained at optimized conditions (Xie *et al.* 2013), which also established that the treatment with solid alkali and active oxygen is an effective pretreatment method for biomass utilization.

The molar ratios of arabinose to xylose (Ara/Xyl) and uronic acid to xylose (Uro/Xyl) are often used as an indication of the degree of linearity and/or branching of hemicellulose (Wedig *et al.* 1987), which is closely associated with the solubility of the polysaccharides (Peng *et al.* 2012). As shown in Table 2, the 0.12 and 0.05 molar ratios of Ara/Xyl in the BSF and PSF, respectively, were higher than those in the BIF (0.04) and PIF (0.03). Similarly, the 0.09 and 0.06 molar ratios of Uro/Xyl in the PSF and BSF, respectively, were also higher than those in the BIF (0.01) and PIF (0.00). The higher molar ratios of Ara/Xyl and Uro/Xyl indicated that the degree of branching of the BSF and PSF was higher than in the BIF and PIF, which resulted in a much higher solubility for the BSF and PSF. This result was consistent with previously published results (Sun *et al.* 2004b; Peng *et al.* 2011b; Guan *et al.* 2015). In a comparison between the molar ratio of Ara/Xyl of bamboo and of other typical biomass, it was found that the molar ratios of Ara/Xyl in the BSF and PSF were lower than that of bagasse and corn stalk (Table 3). This phenomenon suggested that the hemicellulose of bamboo residue is mainly composed of xylan (Shi *et al.* 2012a; Shi *et al.* 2012b).

Table 3. Monosaccharide Composition of the Hemicellulose from Different Materials

Hemicellulose		Sugar composition (%)				Molar ratio ^a	Reference
		Ara	Gal	Glu	Xyl	Ara/Xyl	
Bamboo residue	BSF	9.15	2.34	6.24	76.74	0.120	This study
Bamboo pulp	PSF	1.95	0.51	56.91	36.24	0.050	
Bagasse	H-2	10.49	2.70	20.48	63.93	0.164	Shi <i>et al.</i> (2012b)
Bagasse pulp	H-4	5.50	0.88	12.03	79.92	0.069	
Corn stalk	H ₂	12.26	5.17	16.09	62.89	0.195	Shi <i>et al.</i> (2012a)
Corn stalk pulp	H ₄	4.54	1.27	16.54	76.18	0.060	

^a Expressed in relative molar percentages

Chemical Bonds in the Molecules of the Hemicellulose Fractions

As shown in Fig. 3, the FT-IR spectra of the four hemicellulose fractions presented similar absorption bands of typical polysaccharides, which indicated that the four hemicellulose fractions shared similar structures. The typical functional groups and FT-IR signals corresponding to the possible compounds are listed in Table 4.

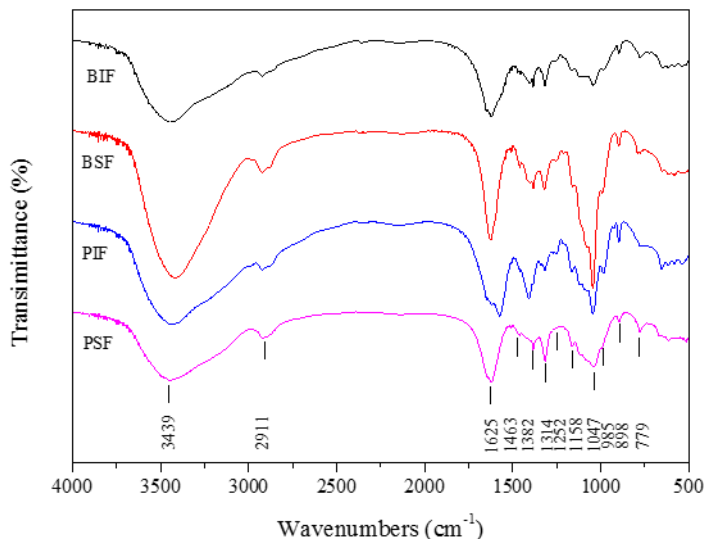


Fig. 3. FT-IR spectra of the four kinds of hemicellulose fractions

In general, the absorption bands around 3439 and 2911 cm^{-1} can be attributed to OH and C-H stretching vibrations, respectively (Shi *et al.* 2013). In the carbonyl stretching region, the bands between 1659 and 1573 cm^{-1} were assigned to the H-O-H angle vibration (Sun *et al.* 2004a) and contributed to the strong affinity of the hemicellulose to water. The absorption bands in the range from 1200 to 800 cm^{-1} are typical of xylan substituted with arabinose (Pang *et al.* 2012), which demonstrated that the xylan backbone was substituted with arabinose. The most important band at approximately 898 cm^{-1} corresponded to the C₁-H group; this signal is characteristic of β -glycosidic linkages between sugar units. The presence of arabinosyl units in hemicellulosic fractions C₁ and C₂, were identified by a low intensity shoulder at 1158 and 985 cm^{-1} (Sun *et al.* 2005). In all of the spectra, a sharp band at 1047 cm^{-1} was assigned to the stretching and bending vibrations of C-O, C-C, C-OH, and glycosidic C-O-C, which are usually regarded as typical features of xylan. This phenomenon indicated that the isolated hemicellulose was mainly composed of xylylans. The results were in agreement with the sugar analysis discussed previously. The signals at 1463 and 1382 cm^{-1} represent C-H, OH, or C-O bending stretch. A weak absorption band at 1252 cm^{-1} related to the C-O linkage in the acetyl group was detected in the BIF, BSF, and PIF and represented the structural feature of acetylation (Peng *et al.* 2011b). However, this signal in the PSF was very weak, which indicated that most of the acetyl groups of the hemicellulose were split off during the cooking process. Additionally, the ester bonds (acetyl, uronic, and ferulic ester groups) were determined to have completely cleaved under the cooking conditions based on the signal disappearance at 1730 to 1740 cm^{-1} in all of the spectra (Sun *et al.* 2004a; Peng *et al.* 2012; Shi *et al.* 2012a). The signal intensity in the BIF, BSF, and PIF was stronger than in the PSF, which might have been due to the higher xylose content in the former three, as was determined by the sugar analysis.

Table 4. Main Functional Groups of the Bamboo Residue Hemicellulose

Wavenumbers (cm ⁻¹)	Functional groups	Compounds
3,800 - 3,000	O-H stretch	Hydroxyl group
2,980 - 2,840	C-H stretch	Alkyl
1,659 - 1,573	H-O-H angle vibration	Water
1,463 and 1,382	C-H stretch, OH or C-O bending stretch	Hemicellulose
1,252	C-O linkage in the acetyl group	Acetylation
1,047	C-O, C-C, C-OH and C-O-C stretch	Xylan
1,158 and 985	C ₁ -H, C ₂ -H bend	Arabinoxylan
898	C ₁ -H bend	β -D-Xylose

Distinction of Constitutional Units of Different Hemicellulose Fractions

To investigate the hemicellulose structure change during the pretreatment process, the structure of the BIF, BSF, PIF, and PSF were characterized using ¹H-¹³C HSQC NMR spectroscopy. The NMR spectra of the four hemicellulose fractions are illustrated in Fig. 4, and the assignment of the chemical shift to ¹H and ¹³C of the PSF are listed in Table 5, which was based on reported NMR data (Peng *et al.* 2011a,b; Wen *et al.* 2011; Yuan *et al.* 2011).

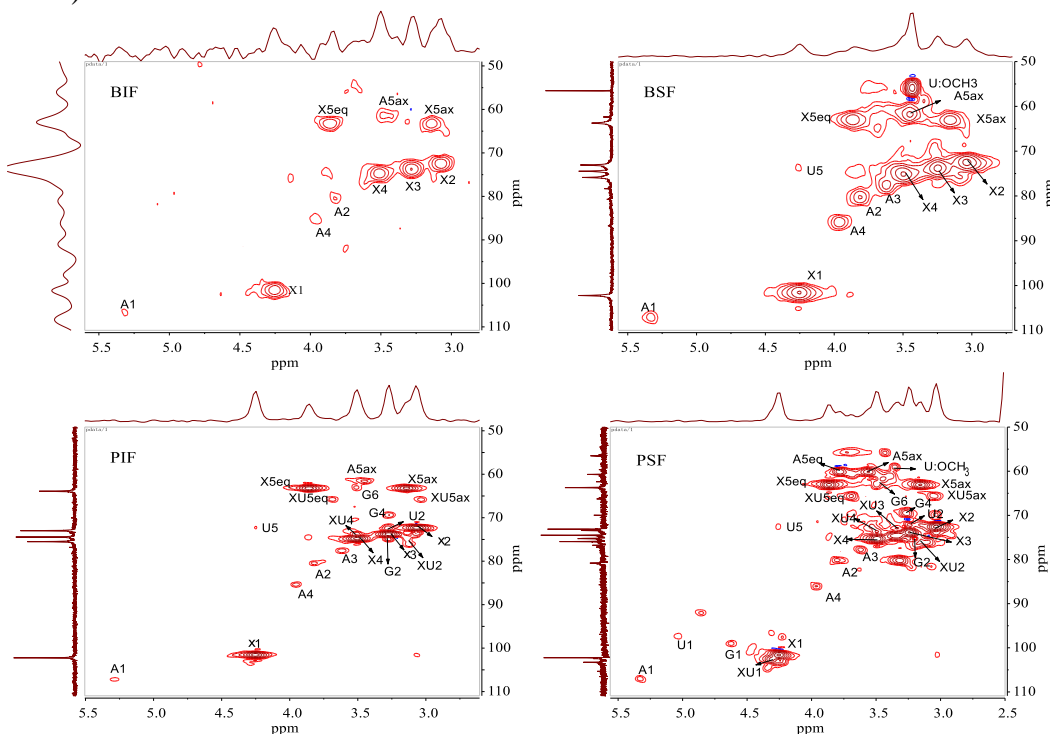


Fig. 4. ¹H-¹³C HSQC spectra of the hemicellulose fractions BIF, BSF, PIF, and PSF. X: (1→4)- β -D-Xylp; A: α -L-Araf; G: (1→4)- β -D-Glucp; U: 4-O-Me- α -D-GlcpA; XU: (1→4)- β -D-Xylp-2-O-(4-O-Me- α -D-GlcpA)

Table 5. ^1H and ^{13}C Chemical Shift (ppm) Assignments for PSF

Glycosyl ^a		Assignments							
		1	2	3	4	5eq ^b	5ax ^c	6	OCH ₃
A	^{13}C	106.95	80.09	77.73	85.98	60.04	60.07	-	-
	^1H	5.33	3.81	3.62	3.97	3.79	3.56	-	-
X	^{13}C	101.57	72.50	73.79	75.24	63.02	63.02	-	-
	^1H	4.26	3.04	3.25	3.50	3.87	3.16	-	-
XU	^{13}C	102.49	76.15	72.12	73.68	65.64	65.56	-	-
	^1H	4.31	3.11	3.25	3.49	3.69	3.05	-	-
G	^{13}C	98.96	75.16	-	69.50	-	-	62.78	-
	^1H	4.63	3.20	-	3.27	-	-	3.50	-
U	^{13}C	97.31	72.24	-	-	-	72.57	-	59.05
	^1H	5.04	3.24	-	-	-	4.26	-	3.36

^a The following designations are used: X: (1→4)- β -D-Xylp; A: α -L-Araf; G: (1→4)- β -D-Glucp; U: 4-O-Me- α -D-GlcpA; XU: (1→4)- β -D-Xylp-2-O-(4-O-Me- α -D-GlcpA); ^b eq: equatorial; ^c ax: axial; - indicated not detected.

As shown in Fig. 4, the signal of (1→4)- β -D-Xylp was clearly observed, and the other signals of α -L-Araf, (1→4)- β -D-Glucp, 4-O-Me- α -D-GlcpA, and (1→4)- β -D-Xylp-2-O-(4-O-Me- α -D-GlcpA) were relatively weak. This phenomenon indicated that (1→4)- β -D-Xylp was the main component in all of the hemicellulose fractions. For the BIF, the main signals were identified to be (1→4)- β -D-Xylp, and the weak signals corresponded to α -L-Araf, but the other signals were very weak or overlapped by signals of (1→4)- β -D-Xylp. This demonstrated that the BIF was comprised of a large amount of (1→4)- β -D-Xylp with less branched chains, especially α -L-Araf, which led to limited solubility. For the BSF, the signals were mainly (1→4)- β -D-Xylp, α -L-Araf, and 4-O-Me- α -D-GlcpA. The latter two signals were noticeably larger in comparison with the BIF, which indicated that the content of the two glycosyl sugars in the BSF was much higher than in the BIF. These results were in accordance with the results of the sugar analysis. For the PIF and PSF, the signals of (1→4)- β -D-Xylp, α -L-Araf, (1→4)- β -D-Glucp, 4-O-Me- α -D-GlcpA, and (1→4)- β -D-Xylp-2-O-(4-O-Me- α -D-GlcpA) were detected. However, the signals for the last four structural units in the PSF were much stronger than those in the PIF. These results were verified by the compositional analysis of the different hemicellulose fractions. The signal for (1→4)- β -D-Xylp in the PSF increased compared with that in the BSF, whereas the signals for α -L-Araf and (1→4)- β -D-Glucp in the PSF decreased compared with those in the BSF. This showed that the content of the two glycosyl units in the PSF was lower than in the BSF. These results indicated that the hemicellulose in the PSF was mainly composed of (1→4)- β -D-Xylp after the loss of the glycosyl in α -L-Araf and (1→4)- β -D-

Glucp during the cooking process. Based on the results above, it was concluded that the hemicellulose from the bamboo residue and pulp had a structure mainly composed of a (1→4)- β -D-Xylp backbone substituted with α -L-Araf and 4-O-methyl- α -D-glucuronic acid. A special phenomenon was seen that the signal for (1→4)- β -D-Glucp was weaker in the PSF spectra than in the BSF based on the signal of OCH₃ at 59.05/3.36 ppm, but there was no significant difference seen in the uronic acid content from the analysis of the monosaccharide compositions. It was speculated that the signal was overlapped by other glycosyl units or was due to poor dissolution. The acetyl groups substituted with xylopyranosyl residues were not found in the spectra of the precipitated hemicellulose, which verified that the acetyl groups were completely cleaved during the pretreatment process.

Thermal Stability of the Different Hemicellulose Fractions

The thermal stability of the four hemicellulose fractions were investigated by TGA and differential thermogravimetric (DTG) analysis. The TGA-DTG curves of the four hemicellulose fractions are illustrated in Fig. 5.

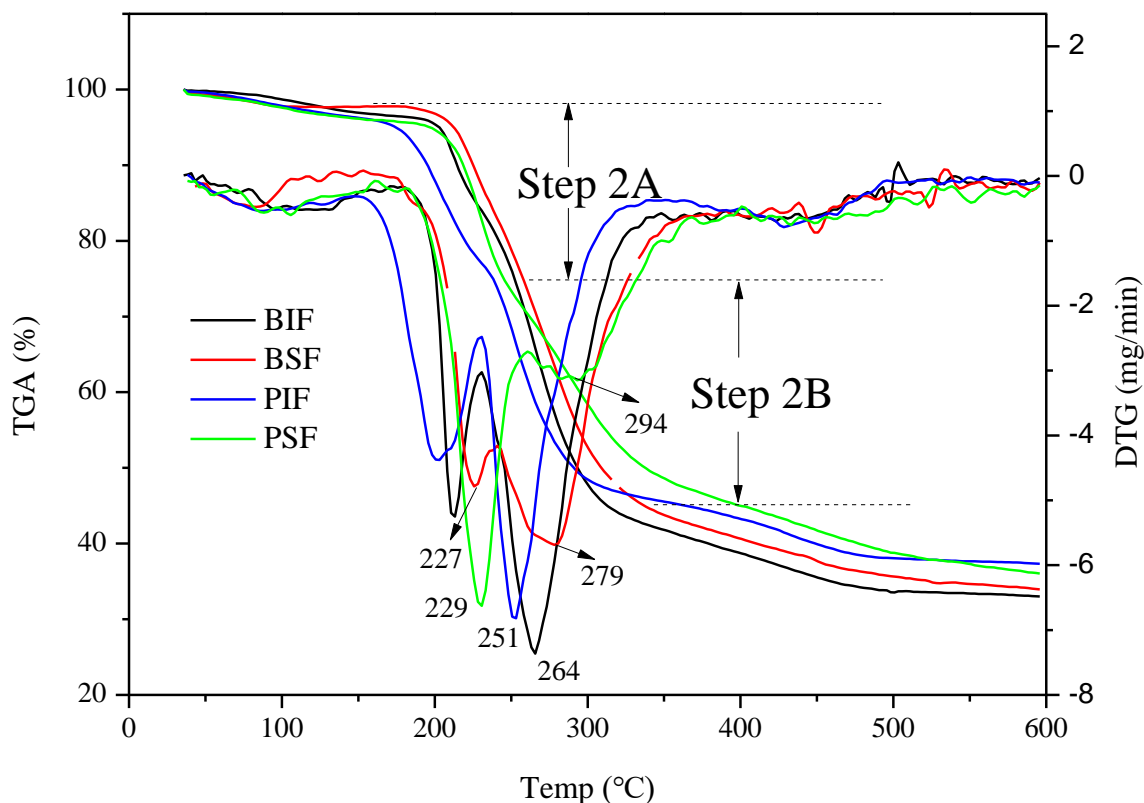


Fig. 5. TGA and DTG curves of the hemicellulose fractions BIF, BSF, PIF, and PSF

As can be seen from the TGA curves, the thermal decomposition of the BIF, BSF, PIF, and PSF appeared to be divided into three weight loss stages. In the first stage, the weight loss observed below 100 °C was attributed to moisture evaporation. In the second stage, the weight loss was observed at 150 to 350 °C and included two decomposition steps, which were labeled Step 2A and Step 2B in Fig. 5. According to Nowakowski and Jones (2008), the first peak, a shoulder on the main degradation peak, was attributed to the low-temperature polymerization process, which results in the formation of char, carbon monoxide, carbon dioxide, and water. The second peak, which occurred at somewhat higher temperatures, was attributed to the generation of volatile anhydrosugars and related monomeric compounds. In the first step, the maximum decomposition rate temperatures for the BIF were higher than for the PIF. Despite similar maximum decomposition rate temperatures for the BSF and PSF, the decomposition rate for the PSF was faster than for the BSF. These results may have been due to the change of bond structures that led to a much looser hemicellulose structure because of the cooking process. In the second step, the same result was obtained for the BIF and PIF. However, the opposite phenomenon occurred for the BSF and PSF, which was possibly related to a large amount of cellulose that had a higher decomposition temperature (321.86 °C) (Kaushik and Singh 2011). Interestingly, the water-soluble fractions (BIF and PIF) showed more thermal stability than the water-insoluble fractions (BSF and PSF) during pyrolysis. Based on the fact that the soluble fractions possessed more branched chains, which led to a higher solubility of the hemicellulose, it was inferred that the arabinose and uronic acid located in the branched chain were liable to form hydrogen bonds with the nearby hemicellulose backbone, resulting in a higher thermal stability. In the course of the third stage, weight loss at a slow decomposition rate was observed at temperatures higher than 350 °C. Approximately 35 wt% of the hemicellulose residues at 600 °C were most likely the end-products from the decomposition of the hemicellulose and salts from the extraction processes (Devallencourt *et al.* 1996).

CONCLUSIONS

1. The CAOSA process was found to be an efficient method capable of destroying the fiber structure of bamboo residue, removing subtotal lignin, and obtaining low-branched xylans that can be further utilized.
2. The molecular structure of the hemicellulose fractions obtained from the bamboo residue and pulp was a (1→4)- β -D-Xylp backbone substituted with α -L-Araf and 4-O-methyl- α -D-glucuronic acid.
3. The water-soluble hemicellulose fractions (BSF and PSF) had a much higher degree of branching than the water-insoluble fractions (BIF and PIF). The fractions of hemicellulose with more side chains presented the tendency to be easily removed from the bamboo residue cell wall during the pretreatment process.
4. The hemicellulose fractions exhibited much lower thermal stabilities after the cooking pretreatment than the raw materials.

ACKNOWLEDGMENTS

The authors are grateful for the financial support from the National Natural Science Foundation of China (NO. 21676223 and NO. 21506177), President Fund of Xiamen University (NO. 20720160087 and NO. 20720160077), the Natural Science Foundation of Fujian Province of China (NO. 2016J01077 and NO. 2015J05034), and the Fujian Provincial Development and Reform Commission, China (NO. 2015489).

REFERENCES CITED

- Bendahou, A., Dufresne, A., Kaddami, H., and Habibi, Y. (2007). "Isolation and structural characterization of hemicelluloses from palm of *Phoenix dactylifera* L.," *Carbohydr. Polym.* 68(3), 601-608. DOI: 10.1016/j.carbpol.2006.10.016
- Blumenkrantz, N., and Asboe-Hansen, G. (1973). "New method for quantitative determination of uronic acids," *Anal. Biochem.* 54(2), 484-489. DOI: 10.1016/0003-2697(73)90377-1
- Devallencourt, C., Saiter, J., and Capitaine, D. (1996). "Characterization of recycled celluloses: Thermogravimetry/Fourier transform infra-red coupling and thermogravimetry investigations," *Polym. Degrad. Stabil.* 52(3), 327-334. DOI: 10.1016/0141-3910(95)00239-1
- Guan, Y., Zhang, B., Qi, X.-M., Peng, F., Yao, C.-L., and Sun, R.-C. (2015). "Fractionation of bamboo hemicelluloses by graded saturated ammonium sulphate," *Carbohydr. Polym.* 129, 201-207. DOI: 10.1016/j.carbpol.2015.04.042
- Huber, G. W., Iborra, S., and Corma, A. (2006). "Synthesis of transportation fuels from biomass: Chemistry, catalysts, and engineering," *Chem. Rev.* 106(9), 4044-4098. DOI: 10.1021/cr068360d
- Jiang, Y., Ding, N., Luo, B., Li, Z., Tang, X., Zeng, X., Sun, Y., Liu, S., Lei, T., and Lin, L. (2017). "Chemical structural change of MgO in the wet oxidation delignification process of biomass with solid alkali," *ChemCatChem* (accepted). DOI: 10.1002/cctc.201700155
- Kaushik, A., and Singh, M. (2011). "Isolation and characterization of cellulose nanofibrils from wheat straw using steam explosion coupled with high shear homogenization," *Carbohydr. Res.* 346(1), 76-85. DOI: 10.1016/j.carres.2010.10.020
- Kim, S. B., Lee, J. H., Oh, K. K., Lee, S. J., Lee, J. Y., Kim, J. S., and Kim, S. W. (2011). "Dilute acid pretreatment of barley straw and its saccharification and fermentation," *Biotechnol. Bioprocess Eng.* 16(4), 725-732. DOI: 10.1007/s12257-010-0305-7
- Leenakul, W., and Tippayawong, N. (2010). "Dilute acid pretreatment of bamboo for fermentable sugar production," *J. Sust. Energ. Environ.* 1(3), 117-120. DOI: 10.1016/j.biortech.2010.08.057
- Liese, W. (1987). "Research on bamboo," *Wood Sci. Technol.* 21(3), 189-209. DOI: 10.1007/BF00351391

- Maekawa, E. (1976). "Studies on hemicellulose of bamboo," *Wood Research: Bulletin of the Wood Research Institute of Kyoto University* 59/60, 153-179.
- Nowakowski, D. J., and Jones, J. M. (2008). "Uncatalysed and potassium-catalysed pyrolysis of the cell-wall constituents of biomass and their model compounds," *J. Anal. Appl. Pyrol.* 83(1), 12-25. DOI: 10.1016/j.jaap.2008.05.007
- Pang, C., Xie, T., Lin, L., Zhuang, J., Liu, Y., Shi, J., and Yang, Q. (2012). "Changes of the surface structure of corn stalk in the cooking process with active oxygen and MgO-based solid alkali as a pretreatment of its biomass conversion," *Bioresource Technol.* 103(1), 432-439. DOI: 10.1016/j.biortech.2011.09.135
- Peng, P., and She, D. (2014). "Isolation, structural characterization, and potential applications of hemicelluloses from bamboo: A review," *Carbohydr. Polym.* 112, 701-720. DOI: 10.1016/j.carbpol.2014.06.068
- Peng, P., Peng, F., Bian, J., Xu, F., Sun, R.-C., and Kennedy, J. F. (2011a). "Isolation and structural characterization of hemicelluloses from the bamboo species *Phyllostachys incarnata* Wen," *Carbohydr. Polym.* 86(2), 883-890. DOI: 10.1016/j.carbpol.2011.05.038
- Peng, P., Peng, F., Bian, J., Xu, F., and Sun, R. (2011b). "Studies on the starch and hemicelluloses fractionated by graded ethanol precipitation from bamboo *Phyllostachys bambusoides* f. shouzhui Yi," *J. Agr. Food Chem.* 59(6), 2680-2688. DOI: 10.1021/jf1045766
- Peng, F., Bian, J., Ren, J.-L., Peng, P., Xu, F., and Sun, R.-C. (2012). "Fractionation and characterization of alkali-extracted hemicelluloses from peashrub," *Biomass Bioenerg.* 39, 20-30. DOI: 10.1016/j.biombioe.2010.08.034
- Ruiz, E., Cara, C., Manzanares, P., Ballesteros, M., and Castro, E. (2008). "Evaluation of steam explosion pre-treatment for enzymatic hydrolysis of sunflower stalks," *Enzyme Microb. Tech.* 42(2), 160-166. DOI: 10.1016/j.enzmictec.2007.09.002
- Scurlock, J., Dayton, D., and Hames, B. (2000). "Bamboo: An overlooked biomass resource?," *Biomass Bioenerg.* 19(4), 229-244. DOI: 10.1016/S0961-9534(00)00038-6
- Shi, J.-B., Yang, Q.-L., Lin, L., Gong, Y., Pang, C.-S., and Xie, T.-J. (2012a). "The structural characterization of corn stalks hemicelluloses during active oxygen cooking as a pretreatment for biomass conversion," *BioResources* 7(4), 5236-5246. DOI: 10.15376/biores.7.4.5236-5246
- Shi, J.-B., Yang, Q.-L., Lin, L., Zhuang, J.-P., Pang, C.-S., Xie, T.-J., and Liu, Y. (2012b). "The structural changes of the bagasse hemicelluloses during the cooking process involving active oxygen and solid alkali," *Carbohydr. Res.* 359, 65-69. DOI: 10.1016/j.carres.2012.06.021
- Shi, J.-B., Yang, Q.-L., Lin, L., and Peng, L.-C. (2013). "Fractionation and characterization of physicochemical and structural features of corn stalk hemicelluloses from yellow liquor of active oxygen cooking," *Ind. Crop. Prod.* 44, 542-548. DOI: 10.1016/j.indcrop.2012.09.026

- Shi, J., Yang, Q., and Lin, L. (2014). "The structural features of hemicelluloses dissolved out at different cooking stages of active oxygen cooking process," *Carbohydr. Polym.* 104, 182-190. DOI: 10.1016/j.carbpol.2014.01.004
- Sun, J., Sun, X., Sun, R., and Su, Y. (2004a). "Fractional extraction and structural characterization of sugarcane bagasse hemicelluloses," *Carbohydr. Polym.* 56(2), 195-204. DOI: 10.1016/j.carbpol.2004.02.002
- Sun, J.-X., Sun, R., Sun, X.-F., and Su, Y. (2004b). "Fractional and physico-chemical characterization of hemicelluloses from ultrasonic irradiated sugarcane bagasse," *Carbohydr. Res.* 339(2), 291-300. DOI: 10.1016/j.carres.2003.10.027
- Sun, X.F., Sun, R.C., Fowler, P., Baird, M.S. (2005). "Extraction and characterization of original lignin and hemicelluloses from wheat straw," *J. Agr. Food Chem.* 53(4), 860–870. DOI: 10.1021/jf040456q
- TAPPI, (1993). "TAPPI Test Methods, T211 om-93, Ash in Wood, Pulp, Paper and Paperboard: Combustion at 525 °C," TAPPI Press, Atlanta
- TAPPI, (2000). "TAPPI Test Methods, T249 cm-00, Carbohydrate Composition of Extractive-free Wood and Wood Pulp by Gas-liquid Chromatography," TAPPI Press, Atlanta
- TAPPI, (2002). "TAPPI Test Methods, T222 om-02. Acid-insoluble Lignin in Wood and Pulp," TAPPI Press, Atlanta
- Wang, L., Fan, X., Tang, P., and Yuan, Q. (2013). "Xylitol fermentation using hemicellulose hydrolysate prepared by acid pre-impregnated steam explosion of corncob," *J. Chem. Technol. Biot.* 88(11), 2067-2074. DOI: 10.1002/jctb.4070
- Wedig, C. L., Jaster, E. H., and Moore, K. J. (1987). "Hemicellulose monosaccharide composition and *in vitro* disappearance of orchard grass and alfalfa hay," *J. Agr. Food Chem.* 35(2), 214-218. DOI: 10.1021/jf00074a012
- Wen, J.-L., Xiao, L.-P., Sun, Y.-C., Sun, S.-N., Xu, F., Sun, R.-C., and Zhang, X.-L. (2011). "Comparative study of alkali-soluble hemicelluloses isolated from bamboo (*Bambusa rigida*)," *Carbohydr. Res.* 346(1), 111-120. DOI: 10.1016/j.carres.2010.10.006
- Wyman, C. E., Dale, B. E., Elander, R. T., Holtzapple, M., Ladisch, M. R., and Lee, Y. Y. (2005). "Coordinated development of leading biomass pretreatment technologies," *Bioresource Technol.* 96(18), 1959-1966. DOI: 10.1016/j.biortech.2005.01.010
- Xie, T., Lin, L., Pang, C., Zhuang, J., Shi, J., and Yang, Q. (2013). "Efficient enzymatic hydrolysis of the bagasse pulp prepared with active oxygen and MgO-based solid alkali," *Carbohydr. Polym.* 94(2), 807-813. DOI: 10.1016/j.carbpol.2013.01.071

- Yang, Q., Shi, J., Lin, L., Zhuang, J., Pang, C., Xie, T., and Liu, Y. (2012). "Structural characterization of lignin in the process of cooking of cornstalk with solid alkali and active oxygen," *J. Agr. Food Chem.* 60(18), 4656-4661. DOI: 10.1021/jf3008663
- Yuan, T.-Q., Sun, S.-N., Xu, F., and Sun, R.-C. (2011). "Characterization of lignin structures and lignin-carbohydrate complex (LCC) linkages by quantitative ^{13}C and 2D HSQC NMR spectroscopy," *J. Agr. Food Chem.* 59(19), 10604-10614. DOI: 10.1021/jf2031549

Article submitted: March 19, 2017; Peer review completed: May 22, 2017; Revised version received and accepted: June 21, 2017; Published: July 3, 2017.

DOI: 10.15376/biores.12.3.5851-5866